Journal of Engineering Physics and Thermophysics, Vol. 71, No. 3, 1998

NUMERICAL STUDY OF THE EDDY MECHANISM OF ENHANCEMENT OF HEAT AND MASS TRANSFER NEAR A SURFACE WITH A CAVITY

S. A. Isaev, A. I. Leont'ev, and
A. E. Usachev

UDC 532.517.4

Based on a solution, by the finite-volume method, of the complete Navier–Stokes and Reynolds equations, with the latter closed by differential equations of a two-parameter dissipative model of turbulence , an analysis is made of the generation of three-dimensional eddy structures in a flow past a surface with a cavity.

The effect of eddy enhancement of heat and mass transfer processes in a flow past surfaces with cavities has become widely known owing to a ten-year series of experimental studies [1-6] conducted by scientific schools in various regions of the former USSR. The generation of waterspout-like eddy structures near surfaces with spherical cavities or a hemispherical cavity on a channel wall, which has been detected in [1, 2], is subjected to a systematic analysis in [4, 5] based on detailed consideration of the unsteady-state mechanism of vortex formation in an isolated cavity under conditions of developed turbulent flow. In [3, 6] it is asserted that formation of large-scale eddy structures in the wall region of a turbulent flow near a surface with spherical cavities permits not only enhancement of heat and mass transfer processes but also a decrease in the hydrodynamic losses associated with liquid flow, in particular, due to a decrease in the friction resistance. However, in [7] the latter statement is called into question because of insufficient experimental justification of it. Moreover, in the same work the method of eddy enhancement of heat and mass transfer processes is related to artificial turbulization of the wall flow. An analysis of the origin of this problem as a whole reveals the need for a more detailed investigation of the governing mechanism of generation of vortices induced owing to concavity reliefs. Therefore, use of methods of numerical simulation seems to be rather expedient owing to the possibility of a detailed diagnosis of the flow field with emphasis of its most important features.

In the past three years numerical simulation of large-scale eddy structures formed in the wall region of laminar and turbulent incompressible-fluid flows in the vicinity of a spherical cavity on a surface has been successively developed [8-12]. The investigations [8, 9] have been carried out in a simplified a formulation under the assumption of symmetry of the unseparated flow relative to the geometric symmetry plane passing through the center of a shallow cavity. In [10] a similar approach is adopted to analyze the vortex structure of the detached flow in a deep cavity, and in [11, 12] results of computer-aided visualization of the vortex flow near a cavity are systematized, including the cases of unsteady development of the process and flow blocking in a thin wall layer.

In our numerical study, considerable attention is paid to a detailed analysis of the governing mechanism of vortex generation in the wall flow of an incompressible viscous fluid near a single spherical cavity on a smooth wall and to an investigation of the influence of the geometric parameters and the operating conditions, including the relative cavity depth and the Reynolds number, on the formation of vortex structures and thedistribution of the flow characteristics.

In our work, use is made of original codes based on a solution of the parabolic Navier–Stokes or Reynolds equations written for Cartesian velocity components and closed in the eddy case with the aid of a two-parameter dissipative model of turbulence. The initial unsteady-state equations in dimensionless form for the generalized variable $\Phi = (u, v, w, k, \varepsilon)$ in the curvilinear nonorthorgonal coordinates ξ, η, ζ are represented as

Academy of Civil Aviation, St. Petersburg, Russia. Translated from Inzhenerno-Fizicheskii Zhurnal, Vol. 71, No. 3, pp. 484-490, May-June, 1998. Original article submitted July 2, 1996.

1062-0125/98/7103-0481$20.00

$$(\Phi J)_t + (U\Phi)_\xi + (V\Phi)_\eta + (W\Phi)_\zeta = JS_\varphi + \left[\frac{\Gamma_\varphi}{J}(D_{11}D_{11} + D_{12}D_{12} + D_{13}D_{13})\Phi_\xi\right]_\xi +$$

$$+ \left[\frac{\Gamma_\varphi}{J}(D_{21}D_{21} + D_{22}D_{22} + D_{23}D_{23})\Phi_\eta\right]_\eta + \left[\frac{\Gamma_\varphi}{J}(D_{31}D_{31} + D_{32}D_{32} + D_{33}D_{33})\Phi_\zeta\right]_\zeta .$$

where the subscripts ξ, η, ζ denote partial derivatives along the coordinate directions. In addition to the source terms proper, S_Φ includes the diffusion terms resulting from the choice of the nonorthogonal coordinate system. The contravariant variables U, V, W responsible for convective transfer through cell faces are calculated as

$$U = D_{11}u + D_{12}v + D_{13}w, \quad V = D_{21}u + D_{22}v + D_{23}w, \quad W = D_{31}u + D_{32}v + D_{33}w.$$

Here, the matrix of the coefficients D_{ij} and the Jacobian J are functions of the Cartesian coordinates.

In calculations of turbulent flows a high-Reynolds-number version of the two-parameter dissipative model of turbulence in combination with the well-known method of near-wall functions is adopted. This an approach can be used for representation of fully developed turbulent flows [13].

As in [8-12], the problem is solved in a finite calculation region bounded by penetrable reference planes that are perpendicular to the geometric symmetry plane and the solid wall and are sufficiently removed from the cavity. On them and on the upper reference plane, parallel to the wall in a flow, soft boundary conditions (conditions of continuation of the solution [13]) are specified.

Discretization of the initial differential equations is accomplished within the framework of the concept of splitting with respect to physical processes in combination with the finite-volume method applied to the equations, written in the delta form in the so-called E-factor formulation, for increments of dependent variables. Unlike the well-known methods of specifying the calculation pattern for the main variables, related to determination of the Cartesian velocity components at spaced nodes (at the centers of sides of a calculation cell) or at joint nodes (at the centers of cells), use is made of a nontraditional approach based on disposition of the indicated variables at the corners of the cells (the nodes of the calculation grid). In this case, the conditions of adhesion on solid surfaces are rigorously satisfied. The use of superimposed grids automatically leads to the problem of consistency of the velocity and pressure fields. Unlike the well-known Rhee–Chou approach associated with introducing a smoothing unit into the pressure correction block, the procedure proposed by Chen [13] is employed. According to this method, when the mass source is determined in the pressure correction procedure, local mass unbalances are averaged over reference volumes located between nodes of the calculation grid.

Much attention is given to constructing an algorithm for calculation of three-dimensional unsteady-state flows. The procedure of [13] with global iterations used for solving unsteady-state equations has been modified to extend to the solution of steady-state equations of fluid dynamics. In so doing, at each time step iterations are continued to convergence of the momentum equations in the solution blocks together with local iterations in the pressure correction block, constructed using the SIMPLEC procedure.

To ensure high accuracy of calculations in the case of sharp gradients of the governing parameters in approximation of convective terms of the explicit part of the equations, use is made of the quadratic Leonard counterflow scheme, characterized by low scheme diffusion. At the same time, in order to smooth discrepancies, increase the stability of the calculation procedure, and damp possible nonphysical oscillations in the implicit part of the equations, the first-order counterflow approximation is adopted in combination with introduced additional diffusion. The stability of counting is also improved by introducing a pseudotime term in the implicit part of the equation for the increment of the generalized dependent variable. The high computational efficiency of the algorithm is attributable to use of the method of incomplete matrix factorization in the Stone version (SIP) to solve the systems of algebraic equations.

Calculations of three-dimensional eddy flows near a cavity in a plane are made on an AT 486 DX4/100 personal computer. A program developed for graphical visualization of eddy flows with the aid of liquid-particle tracks is used for analysis of large-scale eddy structures. The Reynolds number is varied from 700 to 25,250; its upper bound corresponds to the experimentally specified characteristics, namely, an undisturbed-flow velocity U

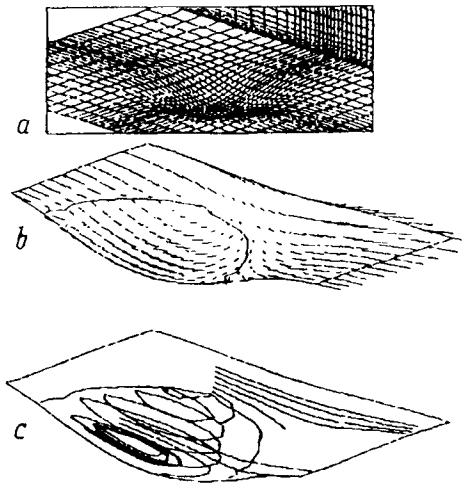

Fig. 1. Fragment of a calculation grid in the vicinity of a cavity with a depth of 0.22 (a); picture of a viscous fluid spreading over a surface with a cavity (b) with the boundary of the detached zone ($u = 0$); structure of an eddy turbulent flow near a cavity at $Re = 10^4$ (c).

= 10 m/sec and a cavity diameter $D = 0.0375$ m. These quantities are used as parameters for nondimensionality in solving the present problem. The depth of the cavity is specified equal to 0.06 and 0.22.

The choice of topology for the three-dimensional calculation grids used to solve the formulated problem is based on specifying a family of grid lines orthogonal to the upper reference boundary (a penetrable plane). In this case, an algebraic oblique grid with a simplified composition and compression of its lines toward the solid wall in the flow and in the region of shear-flow development is generated. Grid nodes are also concentrated in the vicinity of the cavity in order to provide appropriate resolution of the realized eddy structure of the flow. Figure 1a presents a fragment of a calculation grid containing 35 × 18 × 33 nodes. This grid was used to model steady-state detached flows past a deep cavity in laminar and turbulent modes. Calculations of unsteady-state flows were made on 49 × 30 × 47 grids. Grids with a larger number of nodes (61 × 31 × 61) were used for a detailed analysis of the eddy structure of a laminar flow past deep and shallow cavities.

Figure 1b and c presents some results of an investigation of generation of large-seale vortices in a deep cavity for a turbulent flow pattern at $Re = 10^4$. The pictures of the velocity vectors in the wall layer with indication of the return-flow region (Fig. 1b), determined by the line of the longitudinal velocity equal to zero ($u = 0$), demonstrate the initiation of liquid circulation in a horizontal plane. Similarly to the experimentally observed [2] steady-state flow, the cavity liquid overflows toward the incoming external flow and forms concentric streams that indicate that the liquid returns to the peripheral region of the cavity and then is drawn back into the latter. The trajectories of liquid particles shown in Fig. 1c illustrate ejection of wall layers of the liquid from the peripheral part of the cavity and swirling of particles in a large-scale vortex. Here, pronounced mass transfer of the liquid entering the cavity to the region adjoining the symmetry plane is observed. In essence, the cavity in the plane acts as a "vacuum cleaner" that draws the wall liquid layers into the cavity and forms a jet flow in the symmetry-plane zone. In [11], attempts are undertaken to control eddy structures in a cavity by installing a low partition parallel to the incoming flow in order to cut off the liquid flowing in from peripheral layers of the cavity. The researchers succeeded in weakening the vortex in one of the cavity halves; however in solving the steady-state problem it turns out to be rather stable and almost does not experience deformation.

Figure 2 demonstrates numerical modeling of a laminar eddy flow developing in a deep cavity for a Reynolds number ranging from 700 to 2500. It should be noted that calculation of laminar flows near a cavity on a plane is done provided that a Pohlhausen profile with a chosen thickness of the boundary layer is specified for the incoming flow. As a rule, the thickness of the boundary layer near the cavity is of the same order of magnitude as the depth of the latter.

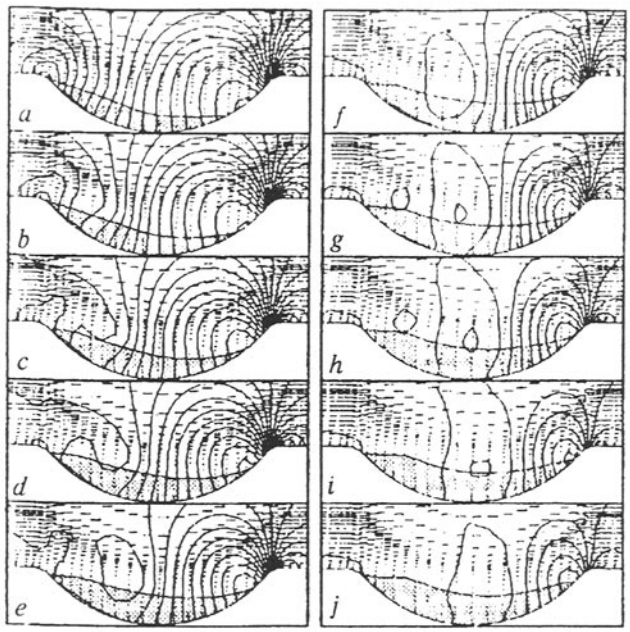

Fig. 2. Evolution of an eddy flow in the longitudinal symmetry plane of a cavity at a Reynolds number ranging from 700 to 2500: pictures of velocity vectors and isobars drawn with a step of 0.01. The line bounding the shaded zone is the isochor corresponding to $u = 0$. Maximum and minimum values of excess pressure referred to the doubled velocity head: a) $t = 0.25$; $p_{max} = 0.11$; $p_{min} = -0.06$; b) 1, 0.11, −0.06; c) 2, 0.1, −0.06; d) 3, 0.1, −0.06; e) 4, 0.09, −0.05; f) 5, 0.08, −0.05; g) 6, 0.08, −0.04; h) 7, 0.06, −0.03; i) 8, 0.05, −0.02; j) 9, 0.04, −0.02. In the figure, dimensionless times determined by the flow velocity and the cavity diameter are given.

The evolution of the pressure fields near the cavity and the deformation of the contours of the detached zone point to a complicated process of flow transformation related to load redistribution and its ultimate equalization. The detached zone tends to occupy the whole cavity, and the intensity of the return flow increases more than twofold (the maximum velocity reaches a value of the order of 0.2). It is pertinent to note that a low (negative) pressure develops at the center of the core vortex. And finally, the drop in the extreme pressures with increasing Reynolds number corresponds to the natural tendency of a decrease in the hydrodynamic resistance of the cavity. Unfortunately, the concept of the occurrence of periodic vortex generation proposed in a number of experimental studies [1, 2, 4, 5] has not yet been confirmed. The large-scale vortex structure in the cavity remains topologically unchanged with the exception of changes in dimensions. This behavior of the eddy flow can be explained by the absence of the considerable disturbances typical for a physical experiment, i.e., the conditions of carrying out a computational experiment turn out to be overly idealized. On the other hand, the instability realized with increase in the Reynolds number, which is capable of triggering destabilization of large-scale eddy flow in the cavity, can exert a considerable influence on the behavior of the flow beyond the Re range considered. In any case, further investigations of the role of an unsteady mechanism in vortex generation are needed, including consideration of a broadened spectrum of geometric factors and conditions affecting the flow structure and turbulent flows.

To analyze steady-state vortex structures generated in cavities in more detail, in Figs. 3, 4 a comparison is made of flows past deep and shallow cavities in a plane for the same thickness of the boundary layer at $Re = 10^3$. The thickness of the boundary layer near the cavities was chosen equal to approximately 0.2. It should be noted that unlike the well-known two-dimensional, in particular, toroidal, vortices, three-dimensional eddy structures require complicated identification. The most suitable holographic methods of flow visualization for the flows considered cases have as yet no computational analogs. Therefore as tools of computer-aided analysis of flows with a complicated spatial structure, to which the flows under consideration pertain, use is made of generators of

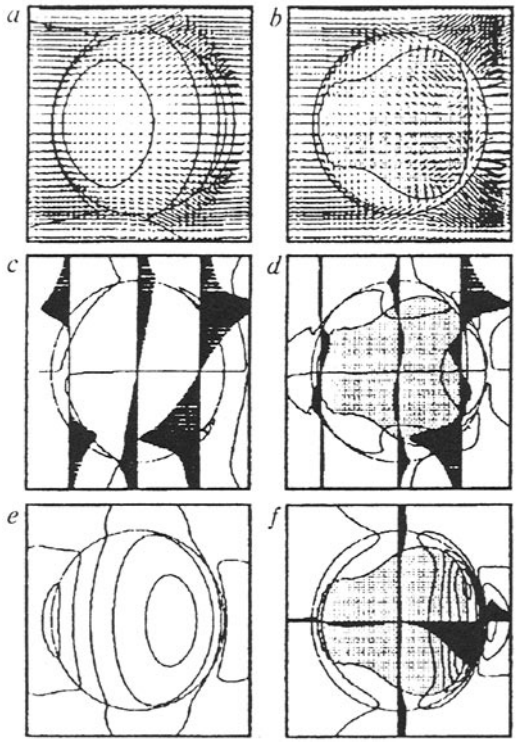

Fig. 3. Comparison of pictures of a viscous fluid spreading over a surface near cavities (a, b), profiles of the transverse velocity (c, d), and isobar pictures (e, f) for cavities with a depth of 0.06 and 0.22 at $Re = 10^3$: a) isotachs from 0.03 to 0.09 with a step of 0.03; b, d, f) contours of the detached zone ($u = 0$); c) isolines w = const corresponding to the values −0.02, 0, 0.02; e, f) isobars from −0.03 to 0.05 and from −0.04 to 0.1, respectively, with a step of 0.02.

pictures of liquid-particle trajectories observed at different viewing angles, slides of pictures of velocity vectors, isolines of scalar parameters representing distinctive plane sections of flow fields in characteristic cross sections of the calculation region, and pictures of liquid spreading over solid surfaces in a flow. In the present work attention focusses on flow pictures and pressure fields on the surface in a flow (Fig. 3) and in a flow cross section running through the cavity center (Fig. 4). In the latter case, pictures of velocity vectors of the so-called secondary flow are constructed using two velocity components, namely, transverse w and vertical v.

As is seen in Fig. 3, a cavity of either depth exerts a retarding action on the wall layers of the liquid; moreover an extensive bulb-like detached zone is formed in the deep cavity. Just as in the flow picture considered in Fig. 1b, the deep cavity exhibits liquid circulation that is drawn from peripheral wall layers and then is displaced toward the incoming flow outside the cavity. It should be noted that the flow coming into the cavity is laminar independently of its depth. At the cavity outlet the wall flow is the same as the flow in a nozzle with an angular semiaperture of up to 45°, i.e., a cavity in a plane abruptly changes the flow direction in the wall layers (Fig. 3a and b).

It is pertinent to note that the profiles of the transverse velocity w are different for shallow and deep cavities due to superposition of eddy structures of different orientation (Fig. 3c and d). They are detected from consideration of the velocity vectors in Fig. 4a and b. It is of interest that the character of the secondary flow in the median plane is completely different for cavities of different depth. Thus, in Fig. 4a a pair of helical vortices is seen to form due to intense mass transfer from the upper liquid layers to the space surrounding the cavity, while in the case of a deep cavity transverse wall streams are formed in the secondary flow that interact in the longitudinal symmetry plane. In the latter case, liquid layers in the cavity and outside it are involved in vortex motion.

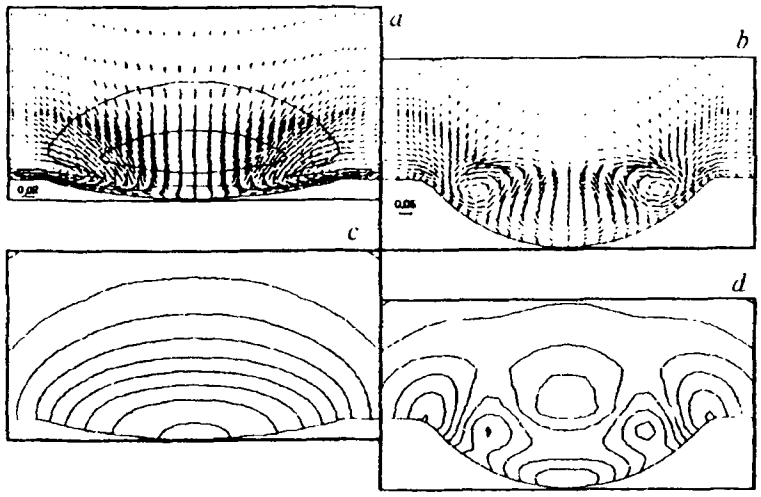

Fig. 4. Pictures of a secondary eddy flow (a, b) and isobars (c, d) in the median cross section of a cavity for two depths of it 0.06 and 0.22 at Re = 10^3: a) isotachs corresponding to 0.01 and 0.02; c, d) isobars from 0.005 to 0.04 with a step of 0.005 and from 0.0025 to 0.0085 with a step of 0.001, respectively.

As is noted in [8, 9], the pressure distribution in a shallow cavity has a canonical dome-like form. This is confirmed by the isobar pictures in Figs. 3e and 4c. For the deep cavity, the pressure distribution exhibits a more complicated and nonuniform character. On the surface in the central part of the cavity the pressure distribution becomes equalized. The elevated-pressure zone deforms and adjoins the site of attachment of the flow, and here two pressure maxima are realized. In the central part of the cavity, an extended region of decreased pressure develops in the shear-layer zone, which is related to the high intensity of the return flow.

To sum up, the conducted numerical study of large-scale vortex structures generated in a cavity in a surface makes it possible to obtain further insight into the mechanism of eddy enhancement of heat and mass transfer processes and to be able to control it.

The work was carried out under financial support of the Russian Fund for Fundamental Research (project No. 96-02-16356). The authors thank Prof. G. A. Dreitser and Prof. A. P. Kozlov for fruitful discussion of the problem.

NOTATION

u, v, w, Cartesian components of the velocity; k, ε, energy of turbulent pulsations and rate of its dissipation; Γ_φ, transfer coefficient; U, V, W, contravariant components of the velocity; p, relative excess pressure; Re, Reynolds number. Subscripts: max, min, maximum and minimum values.

REFERENCES

1. G. I. Kiknadze and Yu. K. Krasnov, Reports of the Academy of Sciences of the USSR, **290**, No. 6, 1315-1319 (1986).
2. P. R. Gromov, A. B. Zobnin, M. I. Rabinovich, and M. M. Sushchik, Pis'ma Zh. Teor. Éksp. Fiz., **12**, No. 21, 1323-1328 (1986).
3. V. N. Afanas'ev, P. S. Roganov, and Ya. P. Chudnovskii, Inzh.-Fiz. Zh., **63**, No. 1, 23-27 (1992).
4. V. S. Kesarev and A. P. Kozlov, Vestnik MGTU, Ser. Mashinostr., No. 1, 106-115 (1993).
5. V. I. Terekhov, S. V. Kalinina, and Yu. M. Mshvidobadze, Rus. J. Eng. Thermophys., 5, 11-34 (1995).
6. V. I. Kosenkov, A. V. Medvedev, and É. D. Sergievskii, in: Heat Transfer Enhancement, Proc. of the 1st Russian National Conference on Heat Transfer, Vol. 8, Moscow (1994), pp. 123-128.

7. G. A. Dreitser, in: Proc. of the 3rd Minsk Int. Heat and Mass Transfer Forum, May 20-24, 1996, Minsk (1996), Vol. 10, Pt. 10, pp. 26-39.
8. V. N. Afanasyev, Ya. P. Chudnovsky, S. A. Isaev, A. I. Leontiev, et al., in: Proc. of the 5th Int. Symp. on Refined Flow Modeling and Turbulent Measurements, Paris (1993), pp. 391-398.
9. S.A. Isaev, V. B. Kharchenko, and Ya. P. Chudnovskii, Inzh.-Fiz. Zh., 67, Nos.. 5-6, 373-378 (1994).
10. S. A. Isaev and Ya. P. Chudnovskii, in: Heat Transfer Enhancement, Proc. of the 1st Russian National Conference on Heat Transfer, Vol. 8, Moscow (1994), pp. 80-85.
11. S. A. Isaev, in: Abstracts of Papers of the Int. Symposium on Heat Transfer Enhancement in Power Machinery (HTEPM '95), Vol. 2, Moscow (1995), pp. 153-156.
12. S. A. Isaev, A. I. Leontiev, and A. E. Usachev, in: Proc. of the 3rd Minsk Int. Heat and Mass Transfer Forum, May 20-24, 1996, Minsk, Vol 1, Pt. 1 (1996), pp. 33-36.
13. I. A. Belov, S. A. Isaev, and V. A. Korobkov, Problems and Methods of Calculation of Separated Flows of an Incompressible Liquid [in Russian], Leningrad (1989).